NMR Techniques

DOI: 10.1002/anie.200907103

Nuclear Magnetic Resonance Using a Spatial Frequency Encoding: Application to *J*-Edited Spectroscopy along the Sample**

*Nicolas Giraud, Laetitia Béguin, Jacques Courtieu, and Denis Merlet**

Nuclear magnetic resonance provides chemists with a unique insight into molecular structure and dynamics over very wide spatial and time ranges.[1] Unfortunately, in most of the recent applications of NMR, the size of the spin networks that are investigated often remain challenging, even for spectrometers that operate at very high fields, since the overlap of signals, as well as the complexity of their multiplet structure, overwhelm the resolution of the NMR spectra.

In this context, considerable methodological developments have been devoted to the design of multidimensional experiments that aim at simplifying the analytical process. For instance, COSY and *J*-resolved experiments illustrate the extent to which chemical shift and scalar coupling information can be separated, thus allowing a rapid assignment of each proton site, and then a measurement of ^1H–^1H couplings.[2,3] Unfortunately, as hard pulses are used in such experiments, they often give overcrowded spectra as soon as the size of the molecular system increases.

One way to reduce the number of interactions that contribute to the structure of NMR spectra involves the use of semiselective pulses, which allow use of coherences that involve a single spin nucleus; for instance, selective refocusing experiments have opened the way to a site-specific measurement of each interaction from unresolved spectra.[4] However, in this latter case, up to $n(n-1)/2$ selective experiments need to be recorded in order to extract all the couplings out of a network of n fully coupled spins, thus requiring a significantly longer experimental time.

In order to overcome the above-mentioned difficulty, we proposed to run different selective experiments on different parts of the sample, that is, we carried out a parallel acquisition of different experiments using a single-receiver-coil system.[5] For this purpose, we created a spatial frequency encoding[6] of the sample, in a manner similar to magnetic resonance imaging techniques. Application of the principle to menthol is shown in Figure 1.

We simultaneously applied a semiselective $\pi/2$ pulse and a pulsed field gradient along the NMR tube (i.e., a z gradient).

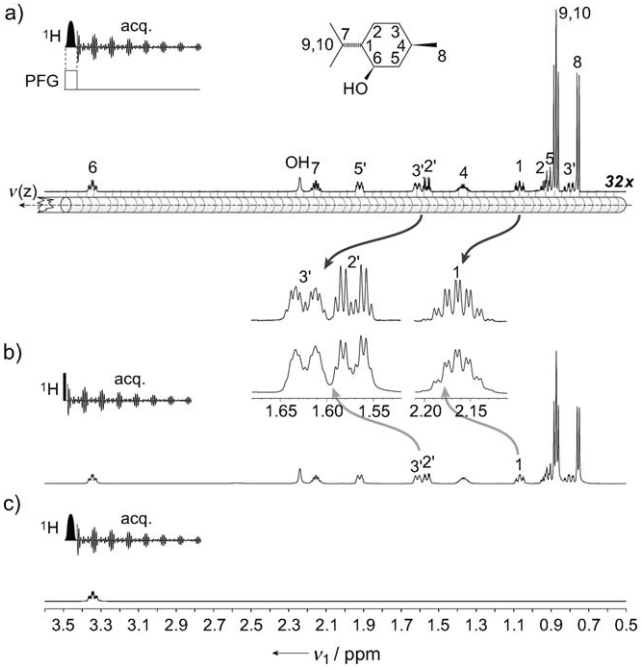

Figure 1. a) Proton spectrum of L-(−)-menthol. The spectrum was acquired using a semiselective pulse (^{1}H channel) applied together with a pulsed z-field gradient (PFG channel). An NMR tube is drawn along the spectrum in order to illustrate the spatial encoding of proton lines according to their resonance frequencies. b) Broadband excitation spectrum, recorded on the same compound. c) Spectrum that results from the application of the semiselective pulse used in (a), at the resonance frequency of proton H^6. The corresponding pulse sequence is shown for each spectrum).

This irradiation scheme can be described as an rf field with a position-dependent offset, and results in the polarization of spin nuclei with different resonance frequencies in different cross sections of the sample. Although the same signals are observed on the gradient-encoded (Figure 1a) and on the broadband excitation spectra of menthol (Figure 1b), the gradient-encoded experiment should actually be compared to the semiselective spectrum (Figure 1c), where one single proton nucleus is excited by the application of a soft pulse over the whole sample. Indeed, the spatial encoding allows this selective experiment to be carried out on each of the proton spins in separate "slices".

We note that each line of the resulting spatially encoded spectrum arises from a restricted cross section of the sample: if the spatial frequency sweep that is induced by the pulsed-field gradient is adjusted so that the width of the spectrum (ca. 3 ppm on menthol) exactly matches the height of the sample, then each signal (whose width can be roughly

[*] Dr. N. Giraud, L. Béguin, Prof. J. Courtieu, Prof. D. Merlet
Laboratoire de RMN en milieu orienté, ICMMO, UMR 8182 CNRS
Univ Paris-Sud 11, bât 410, 91405 Orsay cedex (France)
Fax: (+33) 1-6915-7432
E-mail: denis.merlet@u-psud.fr
Homepage: http://www.icmmo.u-psud.fr/Labos/LRMN/

[**] We thank Prof. James W. Emsley for very helpful discussions.

Supporting information (full experimental procedures about sample preparation, the simulation of a G-SERF experiment on a model spin system, and NMR spectra acquisition) for this article is available on the WWW under http://dx.doi.org/10.1002/anie.200907103.

estimated to 0.1 ppm) is encoded in a cross section that represents 3% of the total sample (hence the 32-fold difference in intensity between the broadband and the encoded spectra in Figure 1). The sensitivity of the resulting experiment thus depends on the strength of the encoding gradient and the selectivity of the pulse, which determine the thickness of the sample region where a multiplet is encoded. However, this spatial restriction leads to the observation of narrower lines on the spatially encoded spectrum, whereas the linewidth in the standard proton spectrum is broader, which is due to the contribution of spatial inhomogeneities along the whole sample.

Gradient-encoded spectroscopy is the cornerstone of ultrafast NMR sequences, which lead to a spectacular reduction of the experimental time in multidimensional experiments.[7] In order to record NMR spectra in a single scan, most recent developments propose to use a frequency sweep in order to encode spin evolution in the indirect domain as an amplitude modulation;[8] that is, different parts of the sample evolve during different time delays t_1. This irradiation scheme is also used to remove undesired coherences (such as zero quantum) from the NMR signal.[9] Our approach is fundamentally different: instead of producing a spatial encoding of a time domain, a frequency (i.e., an offset) encoding is produced in order to individually handle spin coherences along the sample.

Among the numerous probes that can be used to provide data for the determination of 2D or 3D structures of solutes, scalar or dipolar couplings are two of the most informative spin interactions. We have thus applied this methodology to our latest development of the homonuclear SERF pulse sequence,[10] since this kind of encoding paves the way for the improvement of selective refocusing experiments. The resulting G-SERF sequence (gradient-encoded homonuclear selective refocusing spectroscopy; Figure 2), aims to individually assign and measure all the homonuclear couplings between a given proton site S and every other proton I in the spin system within one single 2D experiment.

Figure 3 shows how the G-SERF pulse sequence acts on a system of four fully coupled spins. The first frequency-encoded π/2 pulse excites the proton spins that have different

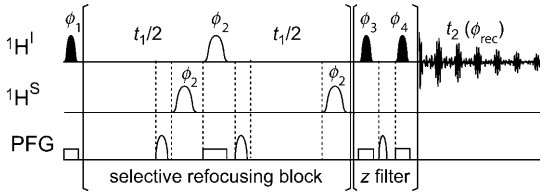

Figure 2. G-SERF pulse sequence. Black and white ellipsoidal shapes on the proton channels $^1H^I$ and $^1H^S$ correspond to π/2- and π-shaped pulses, respectively. The offset of the second, non-encoded π pulse is set to ν^S. White rectangular bars on the pulsed-field gradient (PFG) channel refer to the application of a rectangular-shaped z-field gradient, and the open ellipsoidal shapes to sine-shaped z-field gradients (the latter shapes have been added to select the adequate coherence transfer pathway). Phase cycle: $\phi_1 = (x, -x, x, -x, y, -y, y, -y)$, $\phi_2 = (x, x, -x, -x, y, y, -y, -y)$, $\phi_3 = (x, -x, -x, x, y, -y, -y, y)$, $\phi_4 = (x, -x, y, -y)$, and $\phi_{rec} = (x, -x, -y, y)$.

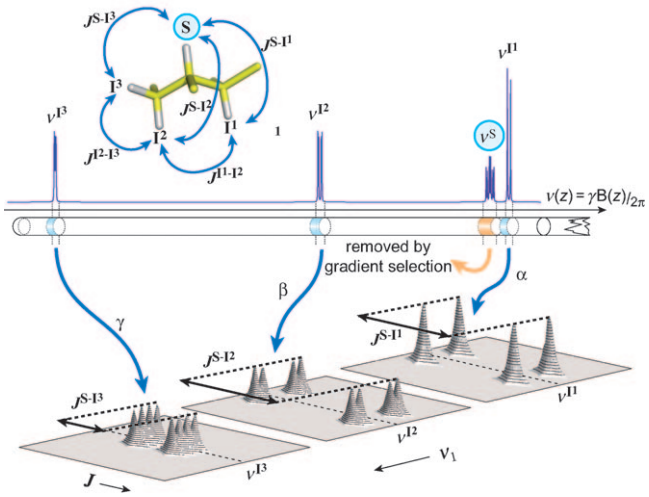

Figure 3. Representation of the effect of the proton G-SERF sequence set for the analysis of the coupling network around S, in a model spin system composed of four coupled protons S, I^1, I^2, and I^3 covalent bonds are displayed as sticks that are colored yellow (around carbon atoms), white (proton), red (oxygen), or blue (nitrogen atoms). In this simulated experiment, each coupling is apparent at the proton chemical shift of the coupling partner I^i ($i = 1$, 2, or 3), and evolves in an individual cross-section of the sample. The resulting spectrum shows correlations at the resonance frequency of each proton I^i, which shows a complex, fully coupled multiplet structure in the direct domain, but appears as a simple doublet with splitting J^{S-Ii} in the indirect domain.

chemical shifts in different cross sections ν^{I1}, ν^S, ν^{I2}, and ν^{I3} of the sample. Then, in each of these cross sections, the selective refocusing block allows every interaction undergone by these protons during t_1, except their coupling with *S*, to be refocused.[10,11] Finally, the free induction decay is acquired during t_2. The resulting spectrum is the sum of the signals originating from every "slice" in the sample, and notably from the three subspectra α, β and γ from the cross sections ν^{I1}, ν^{I2}, and ν^{I3}, which all have a doublet structure in the indirect domain, with splittings J^{S-I1}, J^{S-I2}, and J^{S-I3}, respectively. It is noted that the refocusing of J^{I1-I2} and J^{I2-I3} in the indirect domain brings a great simplification to the multiplet structure. In the cross section ν^S, the signal from the S spins, which does not follow the adequate coherence transfer pathway, is removed by the two selection gradients. This model spin system corresponds to the spin network around proton H^6 in menthol, where the spins S, I^1, I^2, and I^3 can be assigned to H^6, H^1, H^5, and $H^{5'}$ respectively. Figure 4 shows the 2D G-SERF spectrum of menthol for the analysis of the couplings that involve H^6. For H^1, H^5, and $H^{5'}$, doublet signals were observed the splitting of which can be clearly assigned to their respective scalar coupling to H^6. Other proton sites in the molecule that are not coupled to H^6 give singlet signals. This spectrum allows 1) a simple measurement, in the indirect domain, of all the scalar couplings that involve H^6, and 2) a direct assignment, in the direct domain, of the coupling network of H^6, as shown in the molecular structure of menthol (Figure 4).

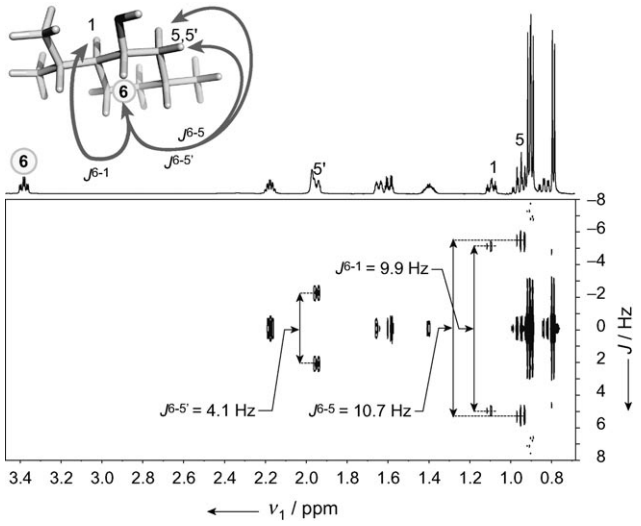

Figure 4. Proton 2D G-SERF spectrum of L-(−)-menthol dissolved in $CDCl_3$. The offset of the non-encoded semiselective pulses is set to the resonance frequency of the proton spin H^6.

We emphasize that the sample spatial encoding offers a novel method for the simplification of correlation spectra and enhancement of resolution compared to standard experiments. As another illustration, the G-SERF experiment was carried out on a sample of strychnine in order to measure the different couplings of the proton 15b (Figure 5a,b). The resulting spectrum clearly shows three doublet signals at the resonance frequencies of the neighboring protons 14, 15a, and 16 (Figure 5c) and singlet signals at all other chemical shifts. We have also acquired a conventional *J*-resolved[2,12] spectrum (Figure 5d). We note that the accurate extraction of any couplings from this latter experiment is a time-consuming task because of 1) the complexity of the multiplets, and 2) the need for a complete analysis of all the signals from the *J*-resolved map, in order to unambiguously assign each coupling (this assignment is in general impossible without recording complementary data such as COSY spectra, which lengthen the overall experimental time needed). Furthermore, the comparison between these two spectra highlights the fact that the doublet splittings in the G-SERF experiment are measured directly on the signal of the coupling partner, hence making the assignment of each interaction straightforward (Figure 6a). This chemical shift information is lost in the *J*-resolved sequence, because of the use of a refocusing hard pulse (Figure 6b). A selective refocusing approach would also allow this assignment issue to be addressed, but at the expense of a much longer experimental time: for n fully coupled, non-equivalent proton sites, up to $n(n-1)/2$ SERF spectra should be acquired in order to gather the measurements of all the scalar couplings. The design of the G-SERF pulse sequence, which allows $(n-1)$ spins to be individually probed, and their coupling to the nth nucleus to be selected, reduces the number of experiments that are required to $(n-1)$. Finally, despite the lower sensitivity inherent to the gradient-encoded spectroscopy, we could record a G-SERF spectrum on strychnine in four hours. Note that the signal-to-noise ratio, which can be observed on the G-SERF data in Figure 6, shows that significantly less concentrated samples could be used. The experimental time is constrained by the need for a high resolution in the indirect dimension, and the number of steps of the phase cycling.

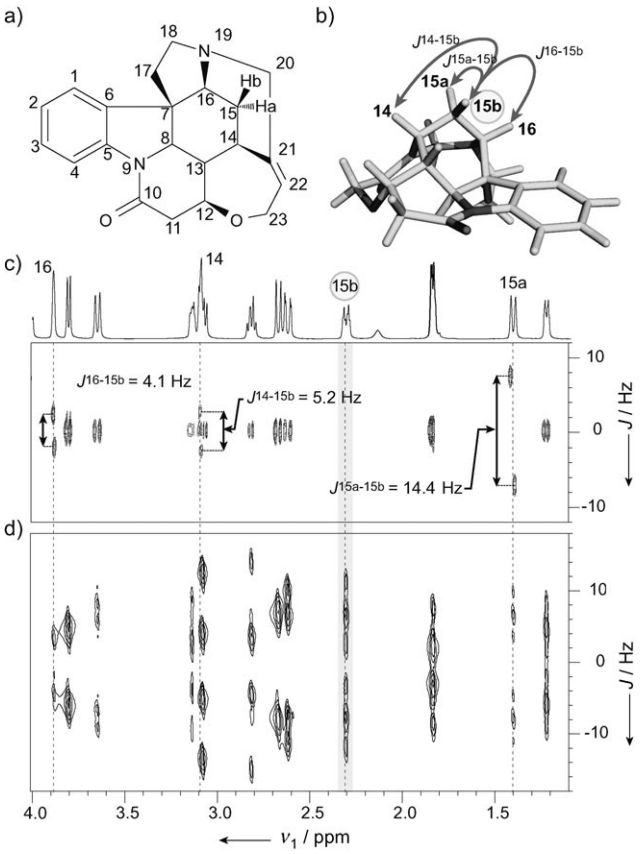

Figure 5. a) Planar structure of strychnine, and b) coupling network around the proton 15b that was probed through a G-SERF 2D experiment. c) ^1H 2D G-SERF spectrum showing the signals of protons 14–16 in strychnine. d) Conventional *J*-resolved spectrum of the same section. The 1D proton spectrum of strychnine is displayed above the G-SERF map.

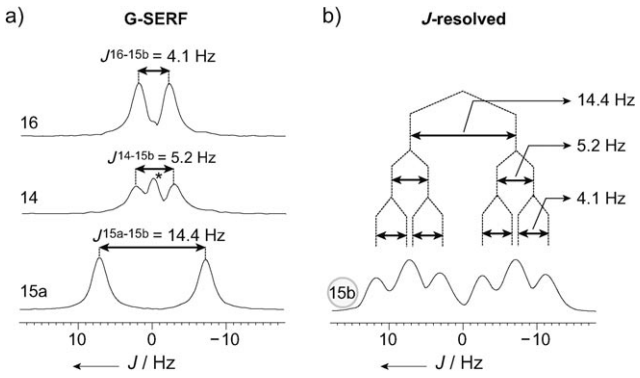

Figure 6. Projections calculated a) from the G-SERF spectrum for the signals of protons 14, 15a, and 16, and, b) from the *J*-resolved experiment for the proton site 15b with detail of the multiplet splitting, which is provided by coupling measurements on the G-SERF data. The signal under the asterisk on the projection of the signal of proton 14 corresponds to the singlet signal of proton 11a (which is not coupled to proton 15b).

In conclusion, we have used the concept of spatial encoding to develop new NMR experiments, which provide a better control of both the number and the lineshape of the correlation peaks obtained from state-of-the-art spectrometers. We have applied this approach to the implementation of a purely *J*-resolved (or *J*-edited) pulse sequence (G-SERF) in a single spectrum, which allows collection, assignment, and selective measurement, in a straightforward and more accurate manner, of the complete homonuclear coupling network around a given proton site in the molecule. Although this technique is less sensitive, it has been shown to provide narrower lines, and can take advantage of the most recent technological progresses (such as cryoprobes), in order to allow the analysis of small quantities in a reasonable experimental time.[13] The potential of this methodology is very wide and is currently being explored by our research group.[14]

Received: December 16, 2009
Published online: April 13, 2010

Keywords: homonuclear coupling · NMR spectroscopy · pulsed-field gradients · spatial encoding

[1] a) A. Abragam in *The Principles of Nuclear Magnetism*, 1st ed., Clarendon Press, Oxford, **1961**; b) C. P. Slichter in *Principles of Magnetic Resonance*, 3rd ed., Berlin, **1990**.
[2] W. P. Aue, J. Karhan, R. R. Ernst, *J. Chem. Phys.* **1976**, *64*, 4226–4227.
[3] a) D. Marion, K. Wüthrich, *Biochem. Biophys. Res. Commun.* **1983**, *113*, 967–974; b) M. Ottiger, F. Delaglio, A. Bax, *J. Magn. Reson.* **1998**, *131*, 373–378; c) B. L. Marquez, W. H. Gerwick, R. T. Williamson, *Magn. Reson. Chem.* **2001**, *39*, 499–530.
[4] a) T. Facke, S. Berger, *J. Magn. Reson. Ser. A* **1995**, *113*, 114–116; b) J. M. Nuzillard, *J. Magn. Reson.* **2007**, *187*, 193–198; c) U. R. Prabhu, B. Baishya, N. Suryaprakash, *J. Phys. Chem. A* **2008**, *112*, 5658–5669.
[5] a) E. Kupce, R. Freeman, B. K. John, *J. Am. Chem. Soc.* **2006**, *128*, 9606–9607; b) P. Nolis, M. Perez-Trujillo, T. Parella, *Angew. Chem.* **2007**, *119*, 7639–7641; *Angew. Chem. Int. Ed.* **2007**, *46*, 7495–7497.
[6] a) K. Zangger, H. Sterk, *J. Magn. Reson.* **1997**, *124*, 486–489; b) A. J. Pell, J. Keeler, *J. Magn. Reson.* **2007**, *189*, 293–299.
[7] a) L. Frydman, A. Lupulescu, T. Scherf, *J. Am. Chem. Soc.* **2003**, *125*, 9204–9217; b) Y. Shrot, L. Frydman, *J. Magn. Reson.* **2008**, *195*, 226–231; c) Y. Shrot, L. Frydman, *J. Chem. Phys.* **2008**, *128*(5), 052209; d) M. Gal, T. Kern, P. Schanda, L. Frydman, B. Brutscher, *J. Biomol. NMR* **2009**, *43*, 1–10.
[8] a) P. Pelupessy, *J. Am. Chem. Soc.* **2003**, *125*, 12345–12350; b) Y. Shrot, B. Shapira, L. Frydman, *J. Magn. Reson.* **2004**, *171*, 163–170; c) P. Pelupessy, L. Duma, G. Bodenhausen, *J. Magn. Reson.* **2008**, *194*, 169–174.
[9] M. J. Thrippleton, R. A. E. Edden, J. Keeler, *J. Magn. Reson.* **2005**, *174*, 97–109.
[10] L. Beguin, N. Giraud, J. M. Ouvrard, J. Courtieu, D. Merlet, *J. Magn. Reson.* **2009**, *199*, 41–47. The G-SERF 2D pulse program is available on our website: http://www.icmmo.u-psud.fr/Labos/LRMN/pp.php.
[11] a) P. Andersson, J. Weigelt, G. Otting, *J. Biomol. NMR* **1998**, *12*, 435–441; b) L. Duma, S. Hediger, A. Lesage, L. Emsley, *J. Magn. Reson.* **2003**, *164*, 187–195; c) S. Cadars, A. Lesage, N. Hedin, B. F. Chmelka, L. Emsley, *J. Phys. Chem. B* **2006**, *110*, 16982–16991.
[12] B. Luy, *J. Magn. Reson.* **2009**, *201*, 18–24.
[13] a) B. Shapira, Y. Shrot, L. Frydman, *J. Magn. Reson.* **2006**, *178*, 33–41; b) Y. Shrot, L. Frydman, *J. Chem. Phys.* **2006**, *125*(20), 204507.
[14] N. Giraud, M. Joos, J. Courtieu, D. Merlet, *Magn. Reson. Chem.* **2009**, *47*, 300–306.

